Jason 3 SLR range correction estimation

Flavien Mercier, Alexandre Couhert

November 8, 2016

1 Introduction

The objective of this document is to analyze the different models used for the Jason 1,2,3 SLR retroreflector range correction (same hardware for the three satellites) and to propose models for this correction, depending on the required performance.

The available corrections in the documentations for Jason 1,2,3 may be very different at some elevations, so it is necessary to do a new analysis of the SLR retroreflector assembly, in order to estimate the precision of these different corrections.

Using the information available in the Jason 3 POD document [ICD POD] a global model is constructed for the SLR retroreflector. This allows to estimate a realistic range correction function. For the Jason SLR retroreflector assembly, it is possible to achieve a sub-millimetric precision using a range correction function of the elevation only. A polynomial expression is proposed here, with a performance better than 2 mm at low elevation, and 0.5 mm at high elevation.

This range correction function is directly compared to the three other available corrections, the differences can reach 5 millimeters at high elevations. These corrections are also verified with a SLR postfit residuals analysis for the first two cycles of Jason 3.

2 Optical path length computation for a corner cube

The figure 1 shows the geometry of the problem for one cube corner. A similar example can be found in [D. Arnold 1979].

O is the optical reference point (corresponding to the complete retroreflector array). C is the center of the external cube corner surface. A is the apex of the cube corner.

l_1 : optical path length for the optical reference point O of the SLR reflector assembly (vacuum propagation). This corresponds to the propagation geometry used in the orbit determination model.

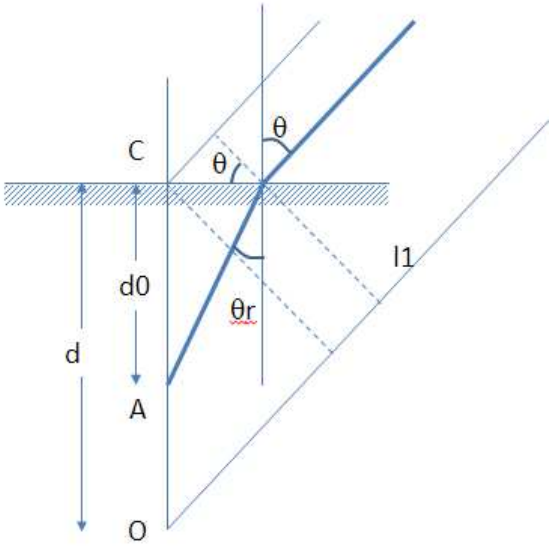

Figure 1: Geometry description

l_2 : optical path length for the ray reflecting at the corner cube apex. This is the measurement (measured propagation time). The diffraction effect [ILRS 2006] is not considered here. The incidence angle is θ and the refraction angle is θ_r, with the relation $\sin\theta = n_\phi \sin\theta_r$. n_ϕ is the refraction index corresponding to the phase velocity at the frequency of the signal. Using n_g for the group refraction index, the expression for l_2 using geometrical optics is (see Appendix) :

$$l_2 = l_1 - d\cos\theta + n_g d_0 cos\theta_r \quad (1)$$

The range correction δl to add to the measurement l_2 to obtain l_1 is :

$$\delta l = d\cos\theta - n_g d_0 cos\theta_r \quad (2)$$

3 SLR array information

The geometry information used here is the POD document [ICD POD], and in the Satellite ICD [ICD SLR]. For the array geometry description, we use the table of the external surfaces coordinates available in the POD document (paragraph 10.1). For the optical center offset relative to the

instrument reference plane, the value is 23.4 mm below the interface (this is not relevant for the array range correction, which is related to the optical center, but is needed to have the correct position on the satellite).

In addition three range corrections are given in paragraph 10.2, corresponding to the directions 0,25,50 degrees in the x0z or yOz plane of the array. The numerical values for the SLR array model are (see the Appendix and [ICD POD]) :

d=82.55 mm for all cubes.

α_0=50 degrees, angle between the central cube and the other cubes reference axes (normal to the external surface).

α_1=34 degrees, angle between two external cubes reference axes.

δl=49.5 mm for the central cube corner correction (0 degree zenith angle).

δl=48.9 mm for 50 degree zenith angle, this value is an average, as the correction depends also on the azimuth in this case.

δl=42.9 mm for 25 degrees zenith angle (this is the point of equal contribution of the two adjacent corner cubes in the xOz plane for example).

We have no description of the cube corner geometry (value of d_0), and also no information on n_g. Assuming that the material is Suprasil quartz glass, we can use the value of $n_g = 1.484$ which is the value used for Saral recent analyses (532 nm) [D. Arnold 2015] and also in [ILRS 2006].

Using the value of the correction δl in the axis of the central cube, and the corresponding distance d, we can derive the product $n_g d_0$ from the equation 2, and then a value for d_0. The values used for the model are thus :

$n_\phi = 1.461$, suprasil phase index of refraction (532 nm).

$n_g = 1.484$, suprasil group index of refraction (532 nm).

$d_0 = 22.3$ mm. This value seems realistic.

4 Complete assembly characteristics

The figure 2 shows the delays δl corresponding to the reflections on the different cubes of the assembly, as a function of the zenith angle θ (relative to the central cube reference direction). This corresponds to the corrections for a ray located in the plane containing the central cube and two external cubes (for example the xOz plane). The blue solid line corresponds to the central cube, the green and red correspond to the two external cubes. For single photon detection, the highest value of the three curves must be used.

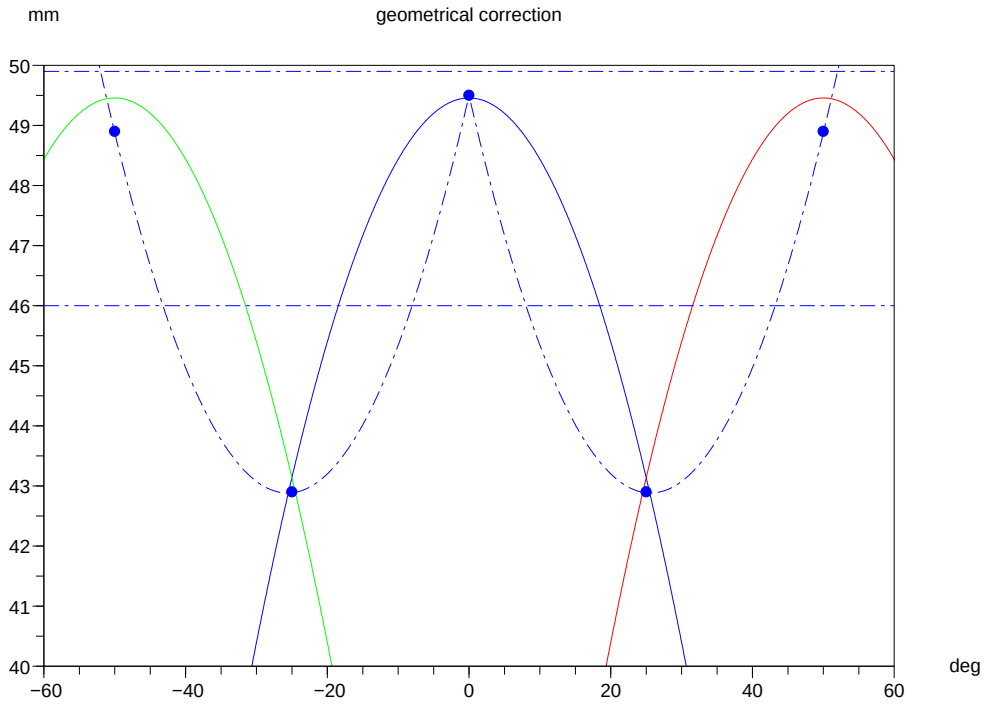

Figure 2: Propagation correction for a plane containing the central cube and two external cubes, dotted lines are the different corrections used for Jason 1,2 or proposed for Jason 3

The symbols on figure 2 correspond to the delay values given in the POD documentation [ICD POD]. For θ=0,-50,50 degrees, this corresponds here to the reference axis of the corner cubes. For θ=-25,25 degrees this is the middle between the two corner cubes, where the delays corresponding to both cubes are identical. What is important here is that the evolution of the correction between these values is now described, even if the used model is not perfect.

The dotted lines correspond to the different corrections used : Jason 1 second degree polynomial expression in $|\theta|$ (curve with the peak at 0 degrees) ; Jason 2, constant value 50.0 mm ; Jason 3, constant value of 46.0 mm.

The problem of these three corrections is that they are biased for high elevation residuals computations which are important for the radial orbit performance verifications (zenith angle below 30 degrees on the station, this corresponds to θ below 24.5 degrees). Usually, at high elevation, the number of measurements close to θ=0 degrees is not very important, so the corrections of Jason 1 will underestimate systematically the correction by 3-4 millimeters, the correction of Jason 2 will overestimate systematically the correction by up to 5 millimeters. The average value of 46.0 mm for Jason 3 seems a good compromise, however the true correction maximal error is +-3 millimeters.

For the higher θ angles, when the active cube is on one external cube, there is a dependency in azimuth. Figure 2 shows the maximum possible value (the ray is directly in the direction of the cube at 50 degrees). Figure 3 shows the correction corresponding to a pointing in a plane containing two external cubes and the optical center (the angle between these cubes is 34 degrees). This means that the correction at 50 degrees is in the interval 46.5 - 49.5 mm.

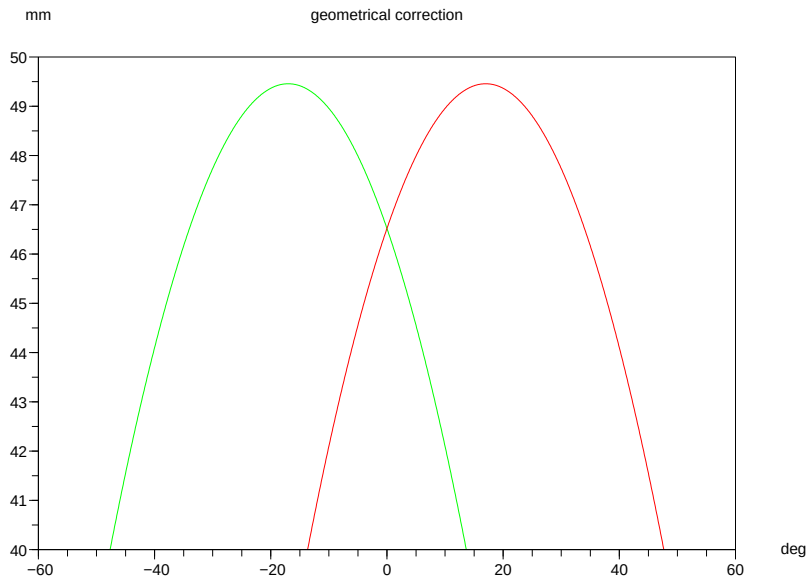

Figure 3: Propagation correction for two external cubes (green and red)

5 Expressions for a range correction function

Different methods are possible :

- use directly the geometrical information to find the corner cube with the normal closest to the incoming direction, and then compute the correction with the formula 2,
- make a table describing the function dependencies in azimuth and zenith angle,
- polynomial expression using the elevation , no azimuth dependency.

The LRA origin in the satellite frame is [1194.0 , 598.0 , 706.2] from [ICD POD].

5.1 Geometrical model

The data are :

$n_\phi = 1.461$

$n_g = 1.484$

Optical centre in LRA reference frame (millimeters) : [0.0 , 0.0 , -23.4]

Geometry

Table 1: Geometry description (millimeters)

Name	1	2	3	4	5	6	7	8	9
d_0	22.3	22.3	22.3	22.3	22.3	22.3	22.3	22.3	22.3
d	82.5	82.6	82.6	82.6	82.6	82.6	82.6	82.6	82.6
normals	0.7661	-0.7661	0.0000	0.0000	0.5417	-0.5417	0.5417	-0.5417	0.0000
	0.0000	0.0000	0.7661	-0.7661	0.5417	0.5417	-0.5417	-0.5417	0.0000
	0.6428	0.6427	0.6428	0.6427	0.6427	0.6427	0.6427	0.6427	1.0000

5.2 Tabulated model

The data are :

Optical centre in LRA reference frame (millimeters) : [0.0 , 0.0 , -23.4]

Corrections, to be added to the measurements, expressed in azimuth (0-360 degrees) and zenith angle (0-65 degrees) (millimeters)

	0	5	10	15	20	25	30	35	40	45	50	55	60	65
0	49.5	49.2	48.4	47.2	45.4	43.1	45.4	47.2	48.4	49.2	49.5	49.2	48.4	47.2
5	49.5	49.2	48.4	47.2	45.4	43.1	45.3	47.1	48.3	49.1	49.3	49.0	48.3	47.0
10	49.5	49.2	48.4	47.2	45.4	43.1	45.0	46.7	47.9	48.6	48.9	48.6	47.8	46.5
15	49.5	49.2	48.4	47.2	45.4	43.1	44.5	46.2	47.3	48.0	48.1	47.8	46.9	45.6
20	49.5	49.2	48.4	47.2	45.4	43.1	43.8	45.4	46.4	47.0	47.1	46.7	45.7	44.3
25	49.5	49.2	48.4	47.2	45.4	43.1	43.8	45.4	46.4	47.0	47.1	46.7	45.7	44.3
30	49.5	49.2	48.4	47.2	45.4	43.1	44.5	46.2	47.3	48.0	48.1	47.8	46.9	45.6
35	49.5	49.2	48.4	47.2	45.4	43.1	45.0	46.7	47.9	48.7	48.9	48.6	47.8	46.5
40	49.5	49.2	48.4	47.2	45.4	43.1	45.3	47.1	48.3	49.1	49.3	49.0	48.3	47.0
45	49.5	49.2	48.4	47.2	45.4	43.1	45.4	47.2	48.4	49.2	49.5	49.2	48.4	47.2
50	49.5	49.2	48.4	47.2	45.4	43.1	45.3	47.1	48.3	49.1	49.3	49.0	48.3	47.0
55	49.5	49.2	48.4	47.2	45.4	43.1	45.0	46.7	47.9	48.7	48.9	48.6	47.8	46.5
60	49.5	49.2	48.4	47.2	45.4	43.1	44.5	46.2	47.3	48.0	48.1	47.8	46.9	45.6
65	49.5	49.2	48.4	47.2	45.4	43.1	43.8	45.4	46.4	47.0	47.1	46.7	45.7	44.3
70	49.5	49.2	48.4	47.2	45.4	43.1	43.8	45.4	46.4	47.0	47.1	46.7	45.7	44.3
75	49.5	49.2	48.4	47.2	45.4	43.1	44.5	46.2	47.3	48.0	48.1	47.8	46.9	45.6
80	49.5	49.2	48.4	47.2	45.4	43.1	45.0	46.7	47.9	48.6	48.9	48.6	47.8	46.5
85	49.5	49.2	48.4	47.2	45.4	43.1	45.3	47.1	48.3	49.1	49.3	49.0	48.3	47.0
90	49.5	49.2	48.4	47.2	45.4	43.1	45.4	47.2	48.4	49.2	49.5	49.2	48.4	47.2
95	49.5	49.2	48.4	47.2	45.4	43.1	45.3	47.1	48.3	49.1	49.3	49.0	48.3	47.0
100	49.5	49.2	48.4	47.2	45.4	43.1	45.0	46.7	47.9	48.6	48.9	48.6	47.8	46.5
105	49.5	49.2	48.4	47.2	45.4	43.1	44.5	46.2	47.3	48.0	48.1	47.8	46.9	45.6
110	49.5	49.2	48.4	47.2	45.4	43.1	43.8	45.4	46.4	47.0	47.1	46.7	45.7	44.3
115	49.5	49.2	48.4	47.2	45.4	43.1	43.8	45.4	46.4	47.0	47.1	46.7	45.7	44.3
120	49.5	49.2	48.4	47.2	45.4	43.1	44.5	46.2	47.3	48.0	48.1	47.8	46.9	45.6
125	49.5	49.2	48.4	47.2	45.4	43.1	45.0	46.7	47.9	48.7	48.9	48.6	47.8	46.5
130	49.5	49.2	48.4	47.2	45.4	43.1	45.3	47.1	48.3	49.1	49.3	49.0	48.3	47.0
135	49.5	49.2	48.4	47.2	45.4	43.1	45.4	47.2	48.4	49.2	49.5	49.2	48.4	47.2
140	49.5	49.2	48.4	47.2	45.4	43.1	45.3	47.1	48.3	49.1	49.3	49.0	48.3	47.0
145	49.5	49.2	48.4	47.2	45.4	43.1	45.0	46.7	47.9	48.7	48.9	48.6	47.8	46.5
150	49.5	49.2	48.4	47.2	45.4	43.1	44.5	46.2	47.3	48.0	48.1	47.8	46.9	45.6
155	49.5	49.2	48.4	47.2	45.4	43.1	43.8	45.4	46.4	47.0	47.1	46.7	45.7	44.3
160	49.5	49.2	48.4	47.2	45.4	43.1	43.8	45.4	46.4	47.0	47.1	46.7	45.7	44.3
165	49.5	49.2	48.4	47.2	45.4	43.1	44.5	46.2	47.3	48.0	48.1	47.8	46.9	45.6
170	49.5	49.2	48.4	47.2	45.4	43.1	45.0	46.7	47.9	48.7	48.9	48.6	47.8	46.5
175	49.5	49.2	48.4	47.2	45.4	43.1	45.3	47.1	48.3	49.1	49.3	49.0	48.3	47.0
180	49.5	49.2	48.4	47.2	45.4	43.1	45.4	47.2	48.4	49.2	49.5	49.2	48.4	47.2
185	49.5	49.2	48.4	47.2	45.4	43.1	45.3	47.1	48.3	49.1	49.3	49.0	48.3	47.0
190	49.5	49.2	48.4	47.2	45.4	43.1	45.0	46.7	47.9	48.7	48.9	48.6	47.8	46.5
195	49.5	49.2	48.4	47.2	45.4	43.1	44.5	46.2	47.3	48.0	48.1	47.8	46.9	45.6
200	49.5	49.2	48.4	47.2	45.4	43.1	43.8	45.4	46.4	47.0	47.1	46.7	45.7	44.3
205	49.5	49.2	48.4	47.2	45.4	43.1	43.8	45.4	46.4	47.0	47.1	46.7	45.7	44.3
210	49.5	49.2	48.4	47.2	45.4	43.1	44.5	46.2	47.3	48.0	48.1	47.8	46.9	45.6
215	49.5	49.2	48.4	47.2	45.4	43.1	45.0	46.7	47.9	48.7	48.9	48.6	47.8	46.5
220	49.5	49.2	48.4	47.2	45.4	43.1	45.3	47.1	48.3	49.1	49.3	49.0	48.3	47.0
225	49.5	49.2	48.4	47.2	45.4	43.1	45.4	47.2	48.4	49.2	49.5	49.2	48.4	47.2
230	49.5	49.2	48.4	47.2	45.4	43.1	45.3	47.1	48.3	49.1	49.3	49.0	48.3	47.0
235	49.5	49.2	48.4	47.2	45.4	43.1	45.0	46.7	47.9	48.7	48.9	48.6	47.8	46.5
240	49.5	49.2	48.4	47.2	45.4	43.1	44.5	46.2	47.3	48.0	48.1	47.8	46.9	45.6
245	49.5	49.2	48.4	47.2	45.4	43.1	43.8	45.4	46.4	47.0	47.1	46.7	45.7	44.3
250	49.5	49.2	48.4	47.2	45.4	43.1	43.8	45.4	46.4	47.0	47.1	46.7	45.7	44.3
255	49.5	49.2	48.4	47.2	45.4	43.1	44.5	46.2	47.3	48.0	48.1	47.8	46.9	45.6
260	49.5	49.2	48.4	47.2	45.4	43.1	45.0	46.7	47.9	48.7	48.9	48.6	47.8	46.5

265	49.5	49.2	48.4	47.2	45.4	43.1	45.3	47.1	48.3	49.1	49.3	49.0	48.3	47.0
270	49.5	49.2	48.4	47.2	45.4	43.1	45.4	47.2	48.4	49.2	49.5	49.2	48.4	47.2
275	49.5	49.2	48.4	47.2	45.4	43.1	45.3	47.1	48.3	49.1	49.3	49.0	48.3	47.0
280	49.5	49.2	48.4	47.2	45.4	43.1	45.0	46.7	47.9	48.7	48.9	48.6	47.8	46.5
285	49.5	49.2	48.4	47.2	45.4	43.1	44.5	46.2	47.3	48.0	48.1	47.8	46.9	45.6
290	49.5	49.2	48.4	47.2	45.4	43.1	43.8	45.4	46.4	47.0	47.1	46.7	45.7	44.3
295	49.5	49.2	48.4	47.2	45.4	43.1	43.8	45.4	46.4	47.0	47.1	46.7	45.7	44.3
300	49.5	49.2	48.4	47.2	45.4	43.1	44.5	46.2	47.3	48.0	48.1	47.8	46.9	45.6
305	49.5	49.2	48.4	47.2	45.4	43.1	45.0	46.7	47.9	48.7	48.9	48.6	47.8	46.5
310	49.5	49.2	48.4	47.2	45.4	43.1	45.3	47.1	48.3	49.1	49.3	49.0	48.3	47.0
315	49.5	49.2	48.4	47.2	45.4	43.1	45.4	47.2	48.4	49.2	49.5	49.2	48.4	47.2
320	49.5	49.2	48.4	47.2	45.4	43.1	45.3	47.1	48.3	49.1	49.3	49.0	48.3	47.0
325	49.5	49.2	48.4	47.2	45.4	43.1	45.0	46.7	47.9	48.7	48.9	48.6	47.8	46.5
330	49.5	49.2	48.4	47.2	45.4	43.1	44.5	46.2	47.3	48.0	48.1	47.8	46.9	45.6
335	49.5	49.2	48.4	47.2	45.4	43.1	43.8	45.4	46.4	47.0	47.1	46.7	45.7	44.3
340	49.5	49.2	48.4	47.2	45.4	43.1	43.8	45.4	46.4	47.0	47.1	46.7	45.7	44.3
345	49.5	49.2	48.4	47.2	45.4	43.1	44.5	46.2	47.3	48.0	48.1	47.8	46.9	45.6
350	49.5	49.2	48.4	47.2	45.4	43.1	45.0	46.7	47.9	48.6	48.9	48.6	47.8	46.5
355	49.5	49.2	48.4	47.2	45.4	43.1	45.3	47.1	48.3	49.1	49.3	49.0	48.3	47.0
360	49.5	49.2	48.4	47.2	45.4	43.1	45.4	47.2	48.4	49.2	49.5	49.2	48.4	47.2

The figure 4 shows the rows or the columns of the table above.

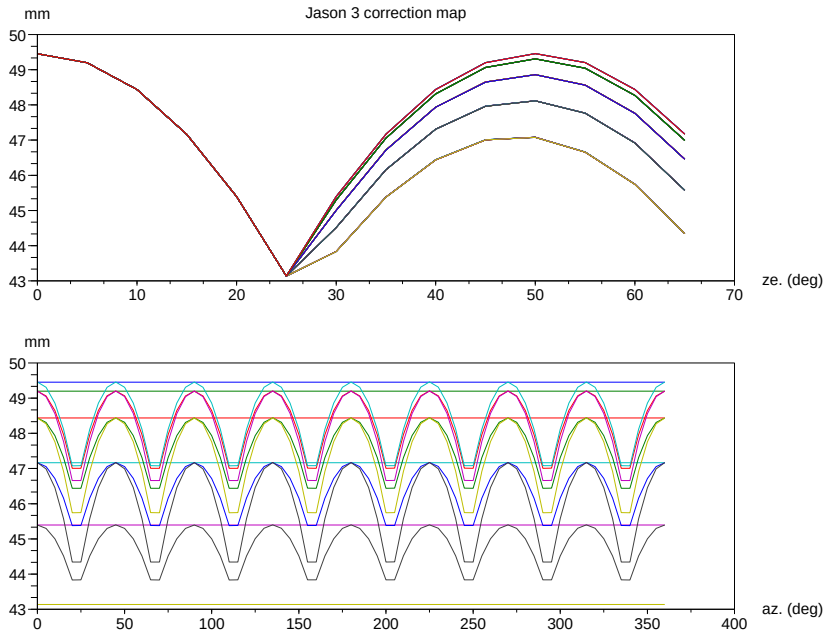

Figure 4: Correction table, dependency in azimuth and zenith angle

5.3 Polynomial expression

Here the objective is to construct a correction suitable for the SLR processing. It is important to have a correct representation of the central part for θ below 25 degrees (see figure 2), and a correct order of magnitude at lower elevations. The current definition in the POD sofware (CNES/Zoom) is a polynomial function of $|\theta|$, so we generate a polynomial expression for the correction. This means an even polynomial (or at least no or a small first order term).

A second degree polynomial represents perfecly the central peak, but is very erroneous for $|\theta|$ above 30 degrees, where the active cube is an external cube. Thus a higher order polynomial is necessary. 2 maxima and 1 minima are needed (see figure 2), so the degree is 4 at least. The figure 5 shows the theoretical correction for different azimuth values (dotted lines for 0,5,10,15 degrees). The correction is common on the central cube, and depends on the azimuth for the contribution of the external cubes. The polynomial corrections are of degree 4 (with or without first degree coefficient) and degree 5 (with null first degree coefficient).

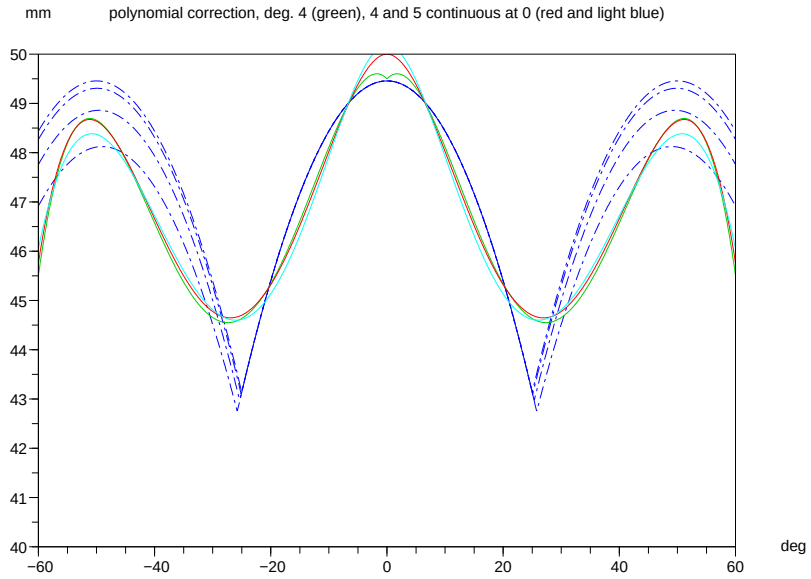

Figure 5: Polynomial correction, reference (blue), deg. 4 (green), 4 and 5 continuous at 0 (red and light blue)

A good fitting is achieved with the degree 4 approximation, with adjusted first degree term, the discontinuity at θ=0 is acceptable. The correction has been minimized for the constributions of the external corner cubes, to take into account the different corrections depending on the azimuth

(table 2).

Table 2: Polynomial range correction coefficients, in meters, for θ in radians

Degree	0	1	2	3	4
4	0.0495	0.0069	-0.1243	0.2480	-0.1328
4 (no deg. 1)	0.0500	0.0	-0.0985	0.2131	-0.1172

Better expressions are possible for an elevation dependent correction. For example looking at figure 5, a function defined with two second degree poynomials, one for θ below 25 degrees (almost no error), and the other for θ above 25 degrees (maximum error 1 mm depending on the azimuth). However, in this case, the geometrical approach described above is simpler and more precise (but a software update is probably needed).

6 Results on cycles 0 and 1 jason 3

The different corrections are tested on the first two cycles of Jason 3. The table 3 shows the mean and rms values for the four available corrections : 2d deg. polynomial (Jason 1), 50 mm (Jason 2), 46 mm (POD documentation Jason 3), 4th deg. polynomial (present study). Two positions for the optical center on the satellite are tested, -23.3 mm corresponds to the POD documentation, -20.2 mm is the value from the ICD.

Table 3: High elevation mean and rms values for cycles 0 and 1 Jason 3, a is for POD documentation optical center, b is for ICD optical center

Case opt. cent.	Cycle 0 a -23.3 mm bias	Cycle 1 a -23.3 mm bias	Cycle 0 a -23.3 mm rms	Cycle 1 a -23.3 mm rms	Cycle 0 b -20.2 mm rms	Cycle 1 b -20.2 mm rms
deg. 2	-3.2	-6.0	10.0	12.5	9.6	11,7
50 mm	2.3	-0.9	9.5	11.1	10.3	11.1
46 mm	-1.7	-4.9	9.4	12.1	9.3	11.4
deg. 4	-0.6	-3.4	9.6	11.5	9.7	11.1

For the mean values (first two columns of table 3), the effect of changing the optical center position of the satellite from -23.3 mm to -20.2 mm is to change the corresponding mean by 2.0 mm. The figure 6 shows the SLR residuals biases for the different configurations. The two cycles have very different overall bias, so it is not possible to choose between the two optical centre offsets values.

The figure 7 shows the rms values. The effect of the optical centre offset is not very important on these rms values. The new polynomial model has a correct behaviour, almost close to the best rms values achieved by the the other formulas.

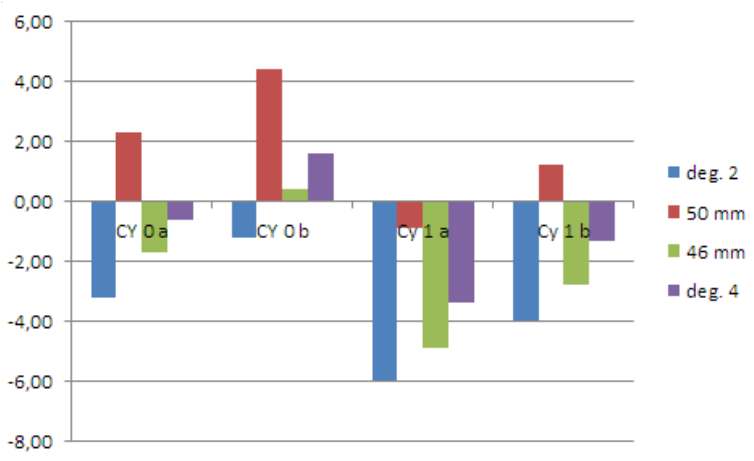

Figure 6: High elevation SLR residuals biases for the different configurations (mm)

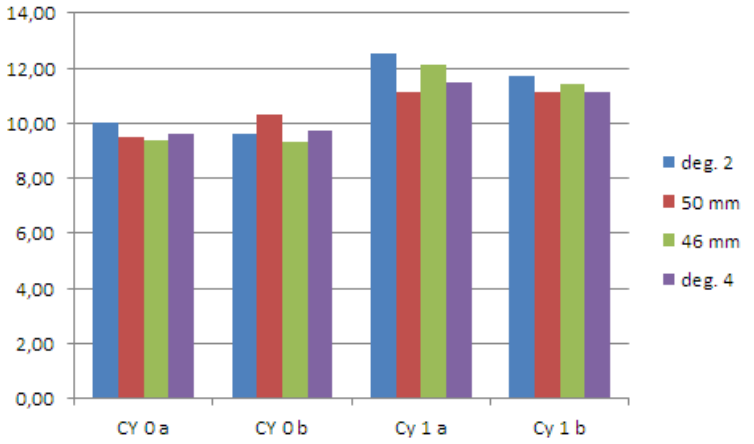

Figure 7: High elevation SLR residuals rms for the different configurations (mm)

To have a clear distinction of the performances of the different correction models, it is necessary to have more data.

7 Conclusion

The complete estimation of the Jason 3 SLR array range correction has been presented (without modelling of the diffraction effects). The results are consistent with the current POD documentation values, and allow to construct a continuous correction for all propagation directions with a better precision than the preceding corrections used on Jason 1 and 2 (same SLR array characteristics).

The tests on the first two cycles of Jason 3 show a correct behaviour of this new correction, but there are not enough measurements to have a good comparison of the performances of the different correction models.

8 Appendix

8.1 range correction expression

Figure 1 shows the geometry of the problem for one cube corner, see for example [D. Arnold 1979]. O is the optical reference point. C is the center of the external cube corner surface. A is the apex of the cube corner. l_1 is the optical path length for the optical reference point O (vacuum propagation). l_2 is optical path length for the ray reflecting at the corner cube apex.

The incidence angle is θ and the refraction angle is θ_r, with the relation $\sin\theta = n_\phi \sin\theta_r$. n_ϕ is the refraction index corresponding to the phase velocity at the frequency of the signal. Using n_g for the group refraction index, the expression for l_2 using geometrical optics is :

$$l_2 = l_1 - d\cos\theta + n_g\frac{d_0}{cos\theta_r} - \frac{d_0}{cos\theta_r}sin\theta_r sin\theta \tag{3}$$

The term $d\cos\theta$ corresponds to a change of the reference point to the center of the corner cube C. The next term is the propagation between the surface of the cube and the apex A, with the refraction index n_g. The last term is the correction for the entry point of the ray in the cube, which has an offset with respect to the center C.

This can be factorized as :

$$\begin{aligned} l_2 &= l_1 - d\cos\theta + n_g\frac{d_0}{cos\theta_r} - \frac{d_0}{cos\theta_r}sin\theta_r sin\theta \\ &= l_1 - d\cos\theta + n_g\frac{d_0}{cos\theta_r} - \frac{d_0}{cos\theta_r}n_\phi \sin^2\theta_r \\ &= l_1 - d\cos\theta + n_g d_0(cos\theta_r + \epsilon) \end{aligned} \tag{4}$$

The term ϵ is usually negligible. It is equal to zero for $n_g = n_\phi$. Practically $(n_g - n_\phi)/n_g$ is small (0.015 for Suprasil), and the maximal value for θ is around 25 degrees (in the Jason 3 array assembly, there is always a cube corner with the incoming direction below 25 degrees from the cube corner axis). ϵ is below 0.004 for the deflections to be considered.

So the range correction δl to add to the measurement l_2 to obtain l_1 can be approximated as :

$$\delta l = d\cos\theta - n_g d_0 cos\theta_r \quad (5)$$

8.2 second order expansion of δl for Jason 3

The numerical values found for Jason 3 are :

$d_0 = 22.3$ mm

$d = 82.55$ mm

$n_\phi = 1.461$

$n_g = 1.484$

d is longer than $n_g d_0$, and θ_r is smaller than θ.

This means that at first order in θ, the correction is equivalent to a positive bias $d - n_g d_0 = 49.5$ mm. The second order term is equivalent to $-\frac{1}{2}(d - \frac{n_g}{n_\phi^2} d_0)\theta^2$, this coefficient is -33.5 mm/rd^2. This explains the polynomial shape of the range correction presented in figure 2.

8.3 Optical centre locations for Jason 3

For the positioning of the assembly on the spacecraft, the value is given in the reference documentation [ICD POD] shown on figure 8. The LRA origin in the satellite frame is [1194.0 , 598.0 , 706.2].

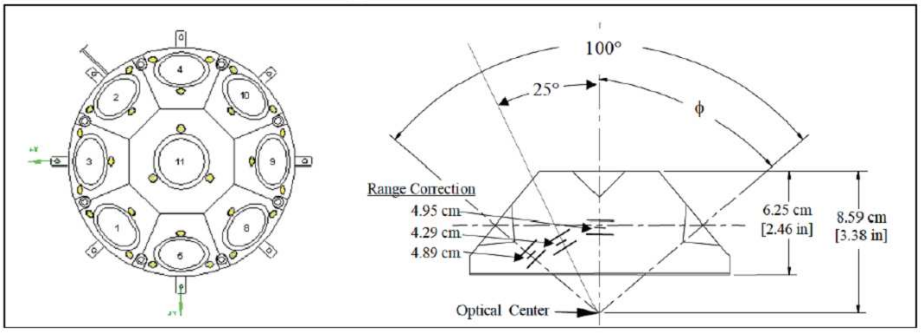

Figure 8: Optical centre location (from [ICD POD])

References

[ICD POD] Jason-3 characteristics for POD processing, V. Couderc, TP4-J0-NT-317-CNES

[ICD SLR] ICD 10176392 Retroreflector Array OSTM/Jason 2

[D. Arnold 1979] Method of calculating retroreflector-array transfer functions. Smithsonian Astrophysical Observatory Special Report No. 382, 1979.

[D. Arnold 2015] Nominal SARAL transfer function, D. Arnold, 2015

[ILRS 2006] ILRS Meeting on retroreflector Arrays, Vienna, April 2006 http://ilrs.gsfc.nasa.gov/docs/2006/retromtg_060406_slides.pdf